BIOCHEMISTRY
including biophysical chemistry & molecular biology
Article

Biochemistry **2010,** *49,* 591–600 591
DOI: 10.1021/bi901546e

The Selenazal Drug Ebselen Potently Inhibits Indoleamine 2,3-Dioxygenase by Targeting Enzyme Cysteine Residues†

Andrew C. Terentis,*[,‖] Mohammed Freewan,[‡,@] Tito S. Sempértegui Plaza,[‖,@] Mark J. Raftery,[§] Roland Stocker,[⊥] and Shane R. Thomas*[,‡]

[‡]*Centre for Vascular Research, School of Medical Sciences, and* [§]*Bioanalytical Mass Spectrometry Facility, University of New South Wales, Sydney, Australia,* [‖]*Department of Chemistry and Biochemistry, Florida Atlantic University, Boca Raton, Florida 33431, and* [⊥]*Centre for Vascular Research, School of Medical Sciences (Pathology) and Bosch Institute, Sydney Medical School, University of Sydney, Sydney, Australia*[@]*These authors made equal contributions to this work.*

Received September 4, 2009; Revised Manuscript Received November 25, 2009

ABSTRACT: The heme enzyme indoleamine 2,3-dioxygenase (IDO) plays an important immune regulatory role by catalyzing the oxidative degradation of L-tryptophan. Here we show that the selenezal drug ebselen is a potent IDO inhibitor. Exposure of human macrophages to ebselen inhibited IDO activity in a manner independent of changes in protein expression. Ebselen inhibited the activity of recombinant human IDO (rIDO) with an apparent inhibition constant of 94 ± 17 nM. Optical and resonance Raman spectroscopy showed that ebselen altered the active site heme of rIDO by inducing a transition of the ferric heme iron from the predominantly high- to low-spin form and by lowering the vibrational frequency of the Fe−CO stretch of the CO complex, indicating an opening of the distal heme pocket. Substrate binding studies showed that ebselen enhanced nonproductive L-tryptophan binding, while circular dichroism indicated that the drug reduced the helical content and protein stability of rIDO. Thiol labeling and mass spectrometry revealed that ebselen reacted with multiple cysteine residues of IDO. Removal of cysteine-bound ebselen with dithiothreitol reversed the effects of the drug on the heme environment and significantly restored enzyme activity. These findings indicate that ebselen inhibits IDO activity by reacting with the enzyme's cysteine residues that result in changes to protein conformation and active site heme, leading to an increase in the level of nonproductive substrate binding. This study highlights that modification of cysteine residues is a novel and effective means of inhibiting IDO activity. It also suggests that IDO is under redox control and that the enzyme represents a previously unrecognized in vivo target of ebselen.

Indoleamine 2,3-dioxygenase (IDO)[1] is a 42−45 kDa intracellular, heme enzyme that catalyzes the initial and rate-limiting step of L-tryptophan (L-Trp) metabolism along the kynurenine pathway (*1*−*3*). IDO catalyzes the oxidative cleavage of the pyrrole moiety of L-Trp to yield *N*-formylkynurenine that then hydrolyzes to kynurenine and formate. Purified IDO is inactive with heme present as ferric iron (Fe^{III}). IDO activation requires the reduction of Fe^{III} to ferrous iron (Fe^{II}) to facilitate the binding of L-Trp and O_2 to the active site heme for formation of the active ternary complex (*1*, *3*).

Recent in vivo studies have established an important role for IDO in immune regulation by promoting immune tolerance via suppression of local T cell responses under various physiological and patho-physiological conditions, including mammalian pregnancy, tumor resistance, autoimmunity, chronic inflammation, and chronic infections (*2*). There is significant interest in identifying low-molecular mass chemical inhibitors of the enzyme in the context of immune escape of certain tumors (*4*). This is because IDO, when expressed by tumor cells or tolerogenic dendritic cells and tumor-associated macrophages, can contribute to a pathological state of immune tolerance toward tumor-associated antigens. Accordingly, inhibition of IDO restores the antitumor immune response and represents an effective adjuvant for chemotherapeutic and immunotherapeutic antitumor strategies (*4*, *5*). The most frequently employed inhibitor of IDO is 1-methyltryptophan. While this competitive substrate inhibitor is bioactive, it is relatively inefficient, exhibiting a K_i of 34 μM (*6*). Therefore, there is interest in the discovery of more potent inhibitors of IDO that exhibit K_i values in the nanomolar range (*7*, *8*).

Our previous studies documented that redox-active agents including nitric oxide (*9*, *10*) and antioxidants (*11*) inhibit IDO

†This work was supported by NHMRC Project Grants 350916 and 568774 (to S.R.T.) and 000371 (to R.S.), a Cure Cancer Australia Project Grant (to S.R.T.), and American Chemical Society Petroleum Research Fund Grant 46549-G4 (to A.C.T.). S.R.T. receives support from NHMRC RD Wright Career Development Award 401113 and the Faculty of Medicine, University of New South Wales. R.S. receives support from an NHMRC Senior Principal Research Fellowship, a University of Sydney Professorial Fellowship, and the University of Sydney Medical Foundation. Mass spectrometry was performed at the Bioanalytical Mass Spectrometry Facility within the Analytical Centre, University of New South Wales. This work was undertaken using infrastructure provided by NSW Government coinvestment in the National Collaborative Research Infrastructure Scheme (NCRIS). Subsidized access to this facility is gratefully acknowledged.

*To whom correspondence should be addressed. S.R.T.: Centre for Vascular Research, School of Medical Sciences, University of New South Wales, UNSW Sydney, NSW 2052, Australia; phone, +61-2-9385 2582; fax, +61-2-9385 1389; e-mail, shane.thomas@unsw.edu.au. A.C.T.: Department of Chemistry and Biochemistry, Florida Atlantic University, Boca Raton, FL 33431; phone, (561) 297-0653; fax, (561) 297-2759; e-mail, terentis@fau.edu.

[1]Abbreviations: CD, circular dichroism; DTT, dithiothreitol; Fe^{II}, ferrous iron; Fe^{III}, ferric iron; IDO, indoleamine 2,3-dioxygenase; IFNγ, interferon-γ; L-Trp, L-tryptophan; MDM, human monocyte-derived macrophage; NO, nitric oxide; MPB, 3-(*N*-maleimidylpropionyl)biocytin; rIDO, recombinant human IDO.

Published on Web 12/15/2009

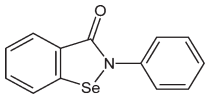

FIGURE 1: Chemical structure of ebselen.

activity in human macrophages. One of the effective agents was the seleno-organic compound ebselen [2-phenyl-1,2-benzisoselenazol-3(2*H*)-one (Figure 1)] that exhibits low toxicity and possesses anti-inflammatory and anti-atherosclerotic properties in vivo (*12*−*15*). Ebselen also exhibits neuroprotective actions in patients after aneurismal subarachnoid hemorrhage and acute ischemic stroke (*16*, *17*). The beneficial properties of ebselen are thought to be related to its glutathione peroxidase activity that reflects its ability to utilize reduced glutathione (GSH) to reduce hydrogen peroxide (H_2O_2) and lipid hydroperoxides (*12*, *13*). Reaction of ebselen with GSH forms ebselen selenylsulfide which in the presence of excess GSH is slowly converted to ebselen selenol and diselenide. Evidence supports the idea that ebselen selenol is primarily responsible for the glutathione peroxidase activity of the drug (*18*, *19*). However, the glutathione peroxidase activity of ebselen is relatively weak (*18*). More recently, ebselen has been identified as an excellent substrate for the thioredoxin/thioredoxin reductase system, and it has been proposed that reaction with this system rather than GSH underlies the antioxidant activity of ebselen in cells (*20*).

Ebselen also exhibits strong electrophilic activity and is therefore capable of forming selenenyl−sulfide bonds with cysteine residues of proteins (*21*, *22*). Accordingly, treatment of cells with ebselen induces a significant decrease in the content of intracellular protein thiols (*22*). The ability of ebselen to covalently react with protein cysteine residues is thought to explain why the selenazal drug modulates the activity of various inflammatory-related enzymes, including lipoxygenase, nitric oxide synthase, and NADPH oxidase (*21*, *23*, *24*). In this study, we report that ebselen also represents a potent inhibitor of IDO by reacting with enzyme cysteine residues leading to enzyme inhibition through changes to the protein structure and active site heme.

EXPERIMENTAL PROCEDURES

Materials. Ebselen was obtained from Cayman Chemicals. Recombinant human interferon-γ (IFNγ) was from R&D Systems. PD10, NAP5, or PD Minitrap G-25 gel filtration columns were obtained from GE-Healthcare. 3-(*N*-Maleimidylpropionyl)biocytin (MPB) was from Molecular Probes. Unless indicated otherwise, all other materials were purchased from Sigma-Aldrich and were of the highest purity available. The concentrations of L-Trp and ebselen stocks were routinely determined by their extinction coefficients (ε_{280} = 5.5 mM^{-1} cm^{-1} and ε_{340} = 5.0 mM^{-1} cm^{-1}, respectively).

Cell Culture. Monocytes were isolated from human blood buffy coats (Australian Red Cross Blood Bank) and matured into monocyte-derived macrophages (MDM) by 8−12 days culture in RPMI 1640 medium supplemented with 10% pooled human serum (*11*). Upon maturation, MDM were treated with recombinant human IFNγ (500 units/mL) to induce IDO expression and activity. For all experiments with MDM, the culture medium was supplemented with 200 μM L-Trp and ebselen added at different concentrations from a concentrated DMSO stock [DMSO final concentration of < 0.5% (v/v)].

Western Blotting and Cellular IDO Activity. Western blotting was performed as described previously (*11*) using a mouse monoclonal antibody directed against human IDO generously provided by O. Takikawa (National Institute for Longevity Sciences, National Center for Geriatrics and Gerontology, Obu City, Japan). Cellular IDO activity was assessed by measuring the extent to which L-Trp in the culture medium was converted to kynurenine. L-Trp and kynurenine levels were measured by HPLC (Agilent 1200 HPLC system) with a Hypersil 3 μm ODS C18 column (Phenomenex) eluted with 100 mM chloroacetic acid and 9% acetonitrile (pH 2.4) at a rate of 0.5 mL/min. L-Trp and kynurenine were detected by UV absorbance at 280 and 364 nm, respectively.

Recombinant Human IDO. Recombinant human IDO (rIDO) encoded by the pQE9-IDO plasmid vector was expressed in *Escherichia coli* as a fusion protein to a hexahistidyl tag and purified as detailed previously (*25*, *26*). The IDO concentration was routinely expressed as the enzyme's heme concentration determined using an extinction coefficient ε_{405} of 159 mM^{-1} cm^{-1}. IDO activity was determined routinely by the ascorbate/methylene blue assay under standard assay conditions (*27*). For activity measurements, rIDO was treated with DMSO vehicle [< 0.5% (v/v)] or ebselen for up to 5 min prior to dilution of rIDO to a final concentration of 50−100 nM into enzyme assay buffer [i.e., 100 mM potassium phosphate buffer (pH 7) containing 0.5 mM EDTA, 25 μM methylene blue, 10 mM sodium ascorbate, 250 μg/mL catalase, and 400 μM L-Trp] and incubation for a further 10 min, after which enzyme activity was assessed by measuring the amount of L-Trp converted to kynurenine by HPLC.

Enzyme Kinetics. The velocity of rIDO enzyme activity was measured by the rate of formation of *N*-formylkynurenine using the ascorbate/methylene blue assay as detailed previously (*28*). For experiments, rIDO (50 nM) was treated with DMSO vehicle [DMSO final concentration of < 1% (v/v)] or the required concentration of ebselen for 5 min followed by addition of enzyme assay buffer [i.e., 100 mM potassium phosphate buffer (pH 7) containing 0.5 mM EDTA, 25 μM methylene blue, 10 mM sodium ascorbate, 250 μg/mL catalase, and 50 μM L-Trp] in a total volume of 0.5 mL in the UV−vis quartz cuvette. Enzyme activity was then measured as the initial rate of formation of *N*-formylkynurenine measured from the slope of the initial linear portion of the increase in absorbance at 321 nm using a Varian Cary 300 spectrophotometer in the time-drive mode.

The enzyme velocity versus ebselen concentration ([ebs]) dose−response curve was fitted to the Morrison equation for tight-binding enzyme inhibitors (eq 1):

$$\frac{v_i}{v_0} = 1 - \Big[([\text{rIDO}] + [\text{ebs}] + K_i^{app} - \sqrt{([\text{rIDO}] + [\text{ebs}] + K_i^{app})^2 - 4[\text{rIDO}][\text{ebs}]}\Big]/(2[\text{rIDO}]) \quad (1)$$

where v_0 is the enzyme velocity in the absence of the inhibitor, v_i is the velocity in the presence of the inhibitor, [rIDO] is the concentration of rIDO enzyme, and K_i^{app} is the apparent inhibition constant under the conditions of study (*29*). Nonlinear data fitting was performed with Origin version 8.

UV−*Visible Spectroscopy*. Optical absorption spectra of Fe^{III}-rIDO (3−10 μM) were recorded with or without ebselen treatment under normal atmospheric conditions in 100 mM potassium buffer (pH 7) using a Varian-Cary 300 spectrophotometer with quartz cuvettes (path length of 1 cm). Fe^{II}-rIDO was

formed by addition of a molar excess of sodium dithionite to vehicle or ebselen-treated rIDO.

Substrate Binding Studies. Substrate binding to rIDO was monitored by the magnitude of the shift of the γ-Soret absorption band maximum in response to the addition of increasing concentrations of L-Trp as previously described (*30*). Absorption spectra for these experiments were recorded with a Varian Cary 3 spectrophotometer in dual-beam mode using quartz sample cuvettes. Samples were prepared in 100 mM potassium phosphate buffer (pH 7) containing 0.5 mM EDTA. For the titrations, aliquots of concentrated L-Trp stocks were cumulatively added to a 4 μM rIDO solution placed in the cuvette. Absorbance changes were corrected for the small dilution factors obtained due to the cumulative addition of the concentrated L-Trp stock. For ebselen-treated rIDO samples, ebselen was added as a concentrated DMSO stock to the buffered enzyme solution at the specified molar ratio [final DMSO concentration of $<1\%$ (v/v)] and incubated for 5 min, and then the sample was passed through a PD Minitrap G-25 column immediately prior to the titration experiment to remove any unbound ebselen. Binding curves were fitted with a standard Langmuir binding isotherm function corresponding to either one or two independent binding sites using Origin version 8.

Resonance Raman (RR) Spectroscopy. Samples of rIDO ($\sim$125 μL, $\sim$30 μM, pH 7) for RR measurements were prepared in a septum-sealed, cylindrical quartz cell. We reduced the samples to the deoxy form by first flushing the sample with argon and then injecting a molar excess of a buffered sodium dithionite solution. Deoxy samples were flushed briefly with carbon monoxide (CO) gas (Airgas Specialty Gases) to form the $Fe^{II}-CO$ complex. The rotating sample cell was irradiated with 4 mW of 413.1 nm light using a mixed krypton/argon ion laser (Spectra Physics, Beamlok 2060). The spectral acquisition time was 5 min. The scattered light was collected at right angles to the incident beam and focused onto the entrance slit (125 μm) of a 0.8 m spectrograph, where it was dispersed by a 600 groove/mm grating and detected by a liquid N_2-cooled CCD camera (Horiba-JY). Spectral calibration was performed against the lines of mercury, silicon, and polystyrene. For ebselen-treated rIDO samples, the drug was added as a concentrated DMSO stock to the buffered enzyme solution at the specified molar ratio [final DMSO concentration of $<1\%$ (v/v)] and incubated for 5 min, and then the sample was passed through a PD Minitrap G-25 column immediately prior to the RR sample preparations and measurements. The final concentration of L-Trp when added was 10 mM.

Circular Dichroism (CD). CD spectra were recorded with a Jasco 810 spectropolarimeter. Samples of rIDO (2 μM) were prepared in 10 mM Tris buffer (pH 7) in a 1 mm path length quartz cuvette. For ebselen-treated rIDO samples, ebselen was added as a concentrated DMSO stock to the buffered enzyme solution at the specified molar ratio [final DMSO concentration of $<1\%$ (v/v)] and incubated for 5 min, and then the sample was passed through a PD Minitrap G-25 column immediately prior to the CD measurement. Spectra were recorded at 20 °C over the range of 260−185 nm with a scan rate of 100 nm/min, a response time of 1 s, and a sensitivity of 100 mdeg. Spectra were acquired from an average of six scans, and all final spectra were corrected for buffer background CD signals. Thermal denaturation curves were acquired by continuously monitoring the CD signal at 222 nm while the sample was heated with a constant temperature ramp rate of 1 °C/min. CD spectra were modeled using CDPro employing the SDP48 data set (*31*, *32*). The reported percent helix values were obtained by averaging the results from SELCON3, CDSSTR, and CONTINLL.

Chemical Labeling of IDO Cysteine Residues. To monitor reactive cysteine residues present on rIDO, we employed the thiol alkylating agent 3-(*N*-maleimidylpropionyl)biocytin (MPB). For this, native or ebselen-treated rIDO (10 μM) was incubated with 1 mM MPB for 30 min prior to addition of SDS loading buffer. Protein samples were then resolved, transferred, and probed with anti-streptavidin (Invitrogen) using Western blotting to assess MPB labeling.

Mass Spectrometry. To assess changes in the molecular mass of rIDO, we employed LC−ESI mass spectrometry. For this, 5 μL samples of native or ebselen-treated rIDO (5 μM) were injected into buffer A (98% H_2O, 2% CH_3CN, and 0.1% formic acid) and reaction products separated using a linear gradient from 5 to 70% buffer B (20% H_2O, 80% CH_3CN, and 0.1% formic acid) at a rate of 150 μL/min using a XDB C18 (5 μm, 2.1 mm × 50 mm) column (Agilent) over 20 min. Solvent was directed to waste for 3 min, and then spectra were acquired using a single quadrupole LC−MS system equipped with an ESI source (MSD1100, Agilent, Palo Alto, CA). Nitrogen was used as nebulizer and drying gas (13 and 7.0 L/min, 300 °C), and samples were ionized at a positive potential of 4000 V and then transferred to the mass analyzer with a fragmentor voltage (capillary to skimmer lens voltage) of 225 V. Spectra were acquired over the mass range of m/z 600−2000 with a cycle time of $\sim$2 s. Each series of multiple charged ions was deconvoluted using the manufacturer's software (Chemstation version A.09.01). The mass accuracy was $\pm$0.05% of the theoretical value.

RESULTS

Ebselen Directly Inhibits Cellular IDO Activity. Our previous study reported that ebselen inhibited IDO activity in human MDM (*11*). To address if the seleno-organic agent inhibits cellular IDO at the level of enzyme activity, we stimulated human MDM with IFNγ for 24 h to induce the expression of active IDO protein, exposed these cells to increasing concentrations of ebselen in fresh, L-Trp-supplemented medium, and then measured the level of IDO protein expression and enzyme activity 4 h later. Ebselen at concentrations of $\leq$100 μM did not alter IDO protein expression yet did inhibit IDO activity, as indicated by the concentration-dependent decrease in the extent to which MDM metabolized L-Trp to kynurenine (Figure 2).

Ebselen Is a Potent Tight-Binding Inhibitor of rIDO. Results from the cellular experiments indicated that ebselen inhibits cellular IDO activity at the post-translational level. We next examined if ebselen also directly inhibited purified rIDO activity by measuring the initial enzyme velocity as a function of ebselen concentration. Pretreatment of rIDO (50 nM) with ebselen for 5 min prior to enzyme activation resulted in a dose-dependent inhibition of activity (Figure 3). Under the experimental conditions employed, $\sim$50% inhibition of enzyme activity was achieved with 200 nM or 4 molar equiv of ebselen (Figure 3). A direct nonlinear least-squares fit of the data using eq 1 (see Experimental Procedures), shown as the solid curve in Figure 3, yielded an apparent inhibition constant (K_i^{app}) for ebselen of 94 $\pm$ 17 nM. As this value is similar to the concentration of total enzyme in the sample (i.e., 50 nM), it is indicative of a tight binding mode of inhibition.

Ebselen Reacts with Cysteine Residues and Alters the Active Site Heme of rIDO To Inhibit Enzyme Activity.

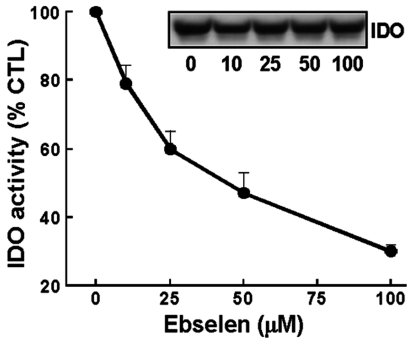

FIGURE 2: Ebselen inhibits cellular IDO activity. Human MDM were treated with IFNγ (500 units/mL) for 24 h prior to being washed and incubated in fresh culture medium supplemented with L-Trp (200 μM) and the indicated concentrations of ebselen. After 4 h, IDO protein and cellular IDO activity were determined as described in Experimental Procedures. IDO activity is expressed as a percentage of the kynurenine formed by control, IFNγ-activated cells (CTL) treated with DMSO vehicle alone. Data shown are means ± the standard error of the mean (SEM) of three independent experiments. The Western blot shown is representative of three independent experiments.

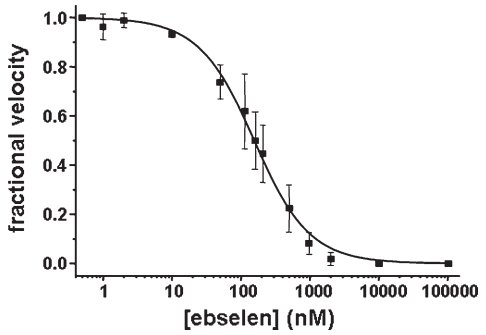

FIGURE 3: Dose−response plot of rIDO enzyme activity vs ebselen concentration. The initial velocity of rIDO-catalyzed L-Trp oxidation was measured following a 5 min pretreatment with varying concentrations of ebselen. The rIDO concentration was 50 nM, and the initial L-Trp concentration was 50 μM. Data points reflect the mean ± standard deviation of triplicate measurements. The fitted curve is generated by a nonlinear least-squares fitting routine using eq 1 as described in Experimental Procedures.

Previous studies indicate that ebselen can inhibit the activity of certain enzymes by reacting with cysteine residues (*21*−*24*). Therefore, we next investigated if ebselen reacts with IDO cysteine residues. Ebselen treatment of rIDO at increasing drug:enzyme molar ratios resulted in a dose-dependent decrease in the level of reactive cysteine residues as assessed by MPB labeling (Figure 4A), and this correlated with the loss of enzyme activity (Figure 4B). Mass spectrometry indicated that treatment of native rIDO with ebselen at drug:enzyme molar ratios of up to 10:1 caused molecular mass additions indicative of ebselen (molecular mass of 274 Da) binding to one to eight cysteine residues of the enzyme depending on the ebselen concentration employed (Figure 5). Treatment of rIDO with ebselen at drug:enzyme molar ratios of >10:1 resulted in maximal binding of eight ebselen molecules to rIDO (data not shown). Of note, ebselen binding to rIDO was heterogeneous; e.g., treatment of rIDO with 6 molar equiv of ebselen resulted in detection of rIDO species with three to seven ebselen molecules attached (Figure 5).

Heme is essential for enzyme activity, and reduction of heme from Fe^{III} to Fe^{II} facilitates the binding of L-Trp and O_2 to the

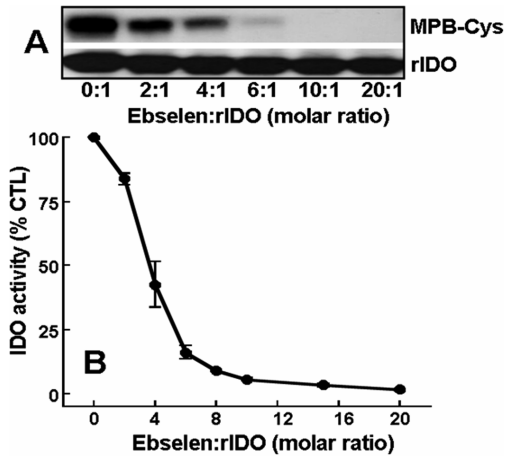

FIGURE 4: Ebselen reacts with cysteine residues of rIDO. rIDO (10 μM) was not treated (0:1) or treated with an increasing number of molar equivalents of ebselen for 5 min before (A) MPB labeling and Western blotting to assess the level of reactive cysteine residues of rIDO and level of IDO protein or (B) dilution into enzyme assay buffer and incubation at 37 °C for 15 min to measure IDO activity. The Western blot is representative of three independent experiments. Enzyme activity is expressed as the percentage of the activity of native, nontreated rIDO (0:1 ebselen:rIDO molar ratio), and data represent the mean ± SEM of four independent experiments.

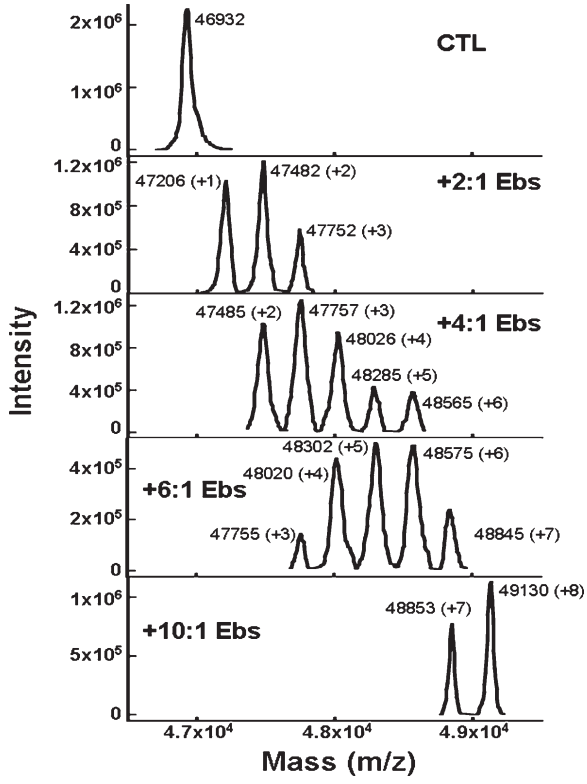

FIGURE 5: Mass spectrometry analysis of rIDO treated with ebselen. rIDO was not treated (CTL) or treated with the indicated number of molar equivalents of ebselen for 5 min before the molecular mass of rIDO was determined by LC−MS analysis as outlined in Experimental Procedures. Mass spectra are representative of three independent experiments.

active-site and the formation of an active quaternary species (*28*). To determine if ebselen perturbs the active site heme of rIDO, we compared the spectral properties of native Fe^{III}-rIDO with that of the ebselen-treated enzyme using UV−visible absorption spectroscopy. Addition of ebselen induced a dose-dependent

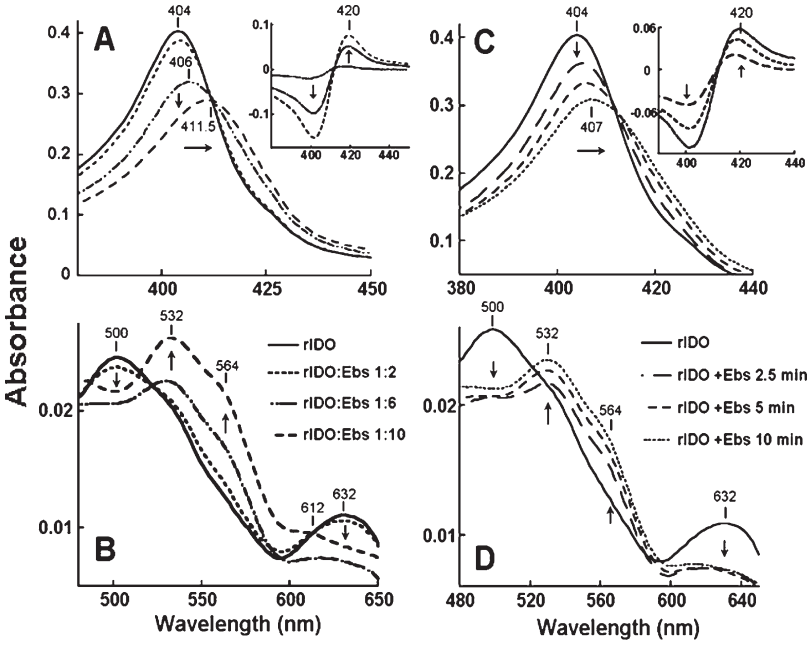

FIGURE 6: Optical spectra of ebselen-treated rIDO. Fe^{III}-rIDO (3−5 μM) was not treated (rIDO) or treated (rIDO and Ebs) with (A and B) ebselen (different numbers of molar equivalents) for 5 min or (C and D) ebselen (6 molar equiv) for 2.5, 5, and 10 min, after which optical absorption spectra were recorded. Spectra are representative of five independent experiments.

(Figure 6A) and time-dependent (Figure 6C) decrease in intensity and red shift of the γ-Soret band from 404 to 411.5 nm. Subtraction of the native from the ebselen-treated, Fe^{III}-rIDO spectrum in the γ-Soret region resulted in a peak with a maximum of ~420 nm (insets, Figure 6A,C). This ebselen-induced red shift is indicative of a transition toward a more low-spin heme iron (*33*). In the α- and β-bands, ebselen induced a dose-dependent (Figure 6B) and time-dependent (Figure 6D) increase in peak intensities at 532, 564, and 612 nm and a decrease in intensities at 500 and 632 nm (Figure 6B,D). In contrast to the Fe^{III} enzyme, ebselen treatment did not significantly alter the optical spectra of Fe^{II}-rIDO, formed by the addition of dithionite to native or ebselen-treated enzyme (data not shown).

We next probed the extent to which the reaction of ebselen with IDO cysteine residues is responsible for the alteration of the active site heme and the inhibitory action of the drug by adding excess GSH to rIDO prior to treatment with ebselen. GSH reacts with ebselen to form glutathione selenyl−sulfide that is subsequently converted into the selenol and diselenide forms of the drug. Excess GSH largely prevented the ability of ebselen to bind to rIDO cysteine residues (Figure 7A), perturb the heme active site (Figure 7B), and inhibit enzyme activity (Figure 7C). We next examined the extent to which breakage of the selenyl−sulfide bonds between ebselen and rIDO cysteine residues abrogated the inhibitory activity of ebselen. Incubation of ebselen-inactivated rIDO with the strong thiol reductant DTT removed the majority of ebselen molecules attached to the enzyme; i.e., rIDO treated with 6 molar equiv of ebselen bound three to seven molecules of the drug, while DTT treatment of this sample resulted in rIDO species with a molecular mass of the native enzyme and with one or two molecules of ebselen attached (Figure 8A). The DTT-induced dissociation of ebselen from rIDO partially restored the optical heme spectrum of native Fe^{III}-rIDO; i.e., while ebselen treatment induced a decrease in the intensity and red shift of the γ-Soret peak of Fe^{III}-rIDO from 404 to 409 nm, removal of the majority of ebselen molecules with DTT treatment induced an increase in the intensity and blue shift of the γ-Soret peak to 405 nm (Figure 8B). Importantly, these DTT-induced changes were associated with > 50% restoration of the original enzyme activity (Figure 8C). Together, these data establish that ebselen reacts with IDO cysteine residues and that this is an important reaction for the seleno-organic agent in perturbing the active site heme and inhibiting IDO activity.

Characterization of Ebselen-Induced Alteration of the Active Site Heme Using Resonance Raman Spectroscopy. We next employed RR spectroscopy to gain further insights into how the reaction of ebselen with IDO cysteines perturbs the active site heme of the enzyme. The RR spectrum of human Fe^{III}-rIDO is characteristic of a six-coordinate, mixed high- and low-spin heme iron complex (*26*). Addition of 3 and 5 molar equiv of ebselen to Fe^{III}-rIDO induced a dose-dependent transition from predominantly high-spin to predominantly low-spin as indicated by the increase in the intensity of the ν_3 band at 1507 cm^{-1} and the ν_2 band at 1578 cm^{-1} (Figure 9A). The heme iron of human deoxy Fe^{II}-rIDO is five-coordinate and high-spin (*26*), which did not change with ebselen treatment (Figure 9B).

The RR spectrum of the Fe^{II}−CO rIDO complex indicated a six-coordinate, low-spin heme complex (*26*), which did not change upon addition of 3 or 5 molar equiv of ebselen (data not shown). In the low-frequency region, the RR spectrum of the Fe^{II}−CO rIDO complex exhibited a strong Fe−CO stretching (ν_{Fe-CO}) vibrational band with a maximum at 511 cm^{-1}, as well as a weak Fe−C−O bending (δ_{Fe-C-O}) vibrational band with a maximum at ~580 cm^{-1} (Figure 10A). Addition of 3 and 5 molar equiv of ebselen caused a dose-dependent shift of the ν_{Fe-CO} band to a lower wavenumber maximum of 500 cm^{-1} (Figure 10A).

The RR spectrum of the rIDO Fe^{II}−CO complex with bound L-Trp displayed a strong ν_{Fe-CO} band with a maximum at 537 cm^{-1} and a moderately strong δ_{Fe-C-O} band with a maximum at 591 cm^{-1} (Figure 10B). Thus, the binding of L-Trp to the heme active site caused an upward shift in the peak positions of the Fe−CO stretching and bending bands, as well as an intensity increase of the bending band. Together, these effects

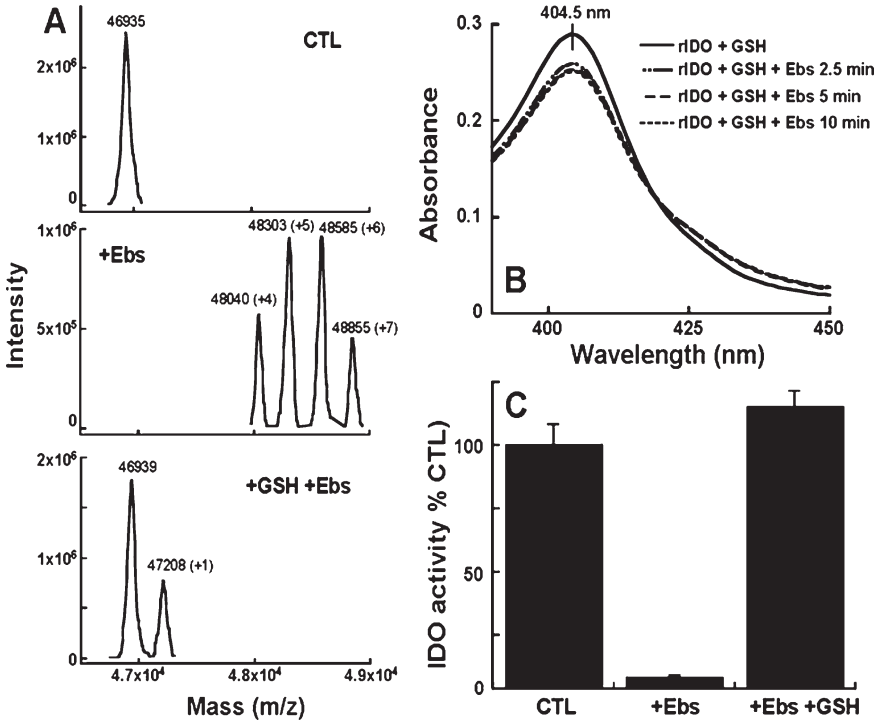

FIGURE 7: GSH protects against ebselen-induced changes in rIDO. rIDO (~3 μM), incubated in the absence or presence of reduced glutathione (1 mM; +GSH), was not treated (CTL) or treated with 6 molar equiv of ebselen (+Ebs) followed by measurement of (A) the molecular mass of rIDO by mass spectrometry 5 min after ebselen treatment, (B) changes in the heme optical absorbance spectrum up to 10 min after ebselen treatment, and (C) enzyme activity after a 5 min ebselen treatment and subsequent dilution into enzyme assay buffer and incubation at 37 °C for a further 15 min. Mass and optical spectra are representative of three independent experiments. Enzyme activity of ebselen-treated rIDO (+Ebs) or ebselen-treated rIDO preincubated with GSH (+GSH+Ebs) is reported as a percentage of the activity of native rIDO or native rIDO incubated with GSH, respectively. Data represent the means ± SEM of three independent experiments.

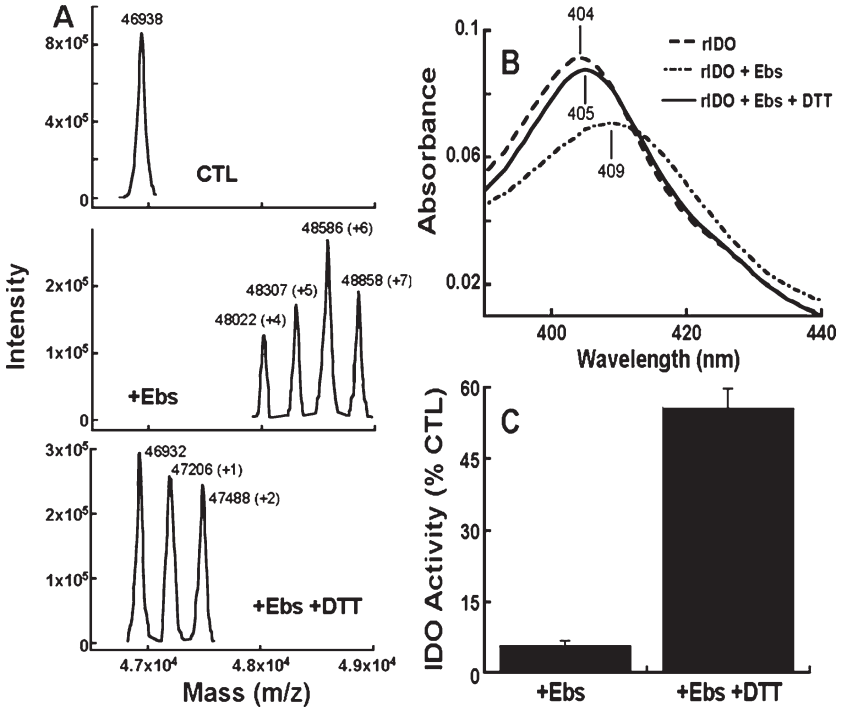

FIGURE 8: Removal of ebselen from rIDO with DTT abrogates the inhibitory action of the selenazal drug. rIDO (~1 μM) was not treated (CTL) or treated with 6 molar equiv of ebselen (+Ebs) for 5 min prior to the determination of (A) the molecular mass of rIDO by mass spectrometry, (B) the heme optical absorbance spectrum, or (C) the enzyme activity. After 5 min, DTT (5 mM) was added to nontreated (CTL+DTT) and ebselen-treated rIDO (+Ebs+DTT) and incubated for 1 h at 37 °C prior to removal of the DTT by gel filtration with a NAP5 column and assessment of (A) the molecular mass of rIDO by mass spectrometry, (B) the heme optical absorbance spectrum, or (C) the enzyme activity. Mass (A) and optical absorbance (B) spectra are representative of three independent experiments. The enzyme activity of ebselen-treated rIDO (+Ebs) or ebselen-treated rIDO incubated with DTT (+Ebs+DTT) is reported as a percentage of the activity of native rIDO (CTL) or native rIDO incubated with DTT (CTL+DTT), respectively. Enzyme activity data represent the means ± SEM of three independent experiments.

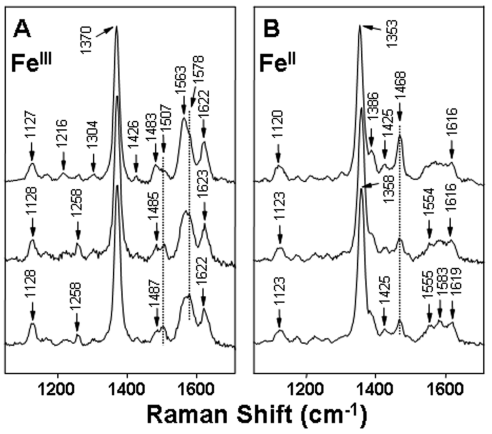

FIGURE 9: Resonance Raman spectra of ebselen-treated rIDO. (A) Spectra of Fe^{III}-rIDO with or without ebselen. The top spectrum is that without ebselen treatment. The remaining spectra correspond to Fe^{III}-rIDO after a 5 min treatment with 3 molar equiv (center) and 5 molar equiv (bottom) of ebselen. (B) Spectra of Fe^{II}-rIDO with or without ebselen. The top spectrum is that without ebselen treatment. The remaining spectra correspond to Fe^{II}-rIDO after a 5 min treatment with 3 molar equiv (center) and 5 molar equiv (bottom) of ebselen. Results are representative of three independent experiments.

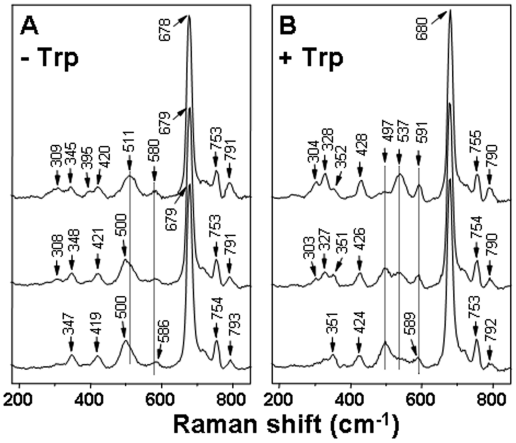

FIGURE 10: Resonance Raman spectra of the ebselen-treated, Fe^{II}−CO rIDO complex. (A) Spectra of the Fe^{II}−CO complex with or without ebselen in the absence of L-Trp. The top spectrum is that without ebselen treatment. The remaining spectra correspond to a 5 min treatment with 3 molar equiv (center) and 5 molar equiv (bottom) of ebselen. (B) Spectra of the Fe^{II}−CO complex with or without ebselen in the presence of L-Trp. The top spectrum is that without ebselen treatment. The remaining spectra correspond to a 5 min treatment with 3 molar equiv (center) and 5 molar equiv (bottom) of ebselen. Results are representative of three independent experiments.

are indicative of tight steric and H-bonding interactions between the substrate L-Trp and the CO distal ligand (*26*). Addition of 3 and 5 molar equiv of ebselen caused a dose-dependent downward shift in the peak position of the ν_{Fe-CO} vibrational band to 497 cm^{-1} and a weakening of the intensity of the δ_{Fe-C-O} band (Figure 10B). These observations support the possibility that the reaction of ebselen with rIDO causes a widening or opening up of the distal pocket, which draws L-Trp and CO apart and weakens their mutual interaction.

Ebselen Enhances the Binding of L-Trp to Fe^{III}-rIDO. We next examined the effect of ebselen treatment on the binding of the substrate L-Trp to Fe^{III}-rIDO. Addition of increasing amounts of L-Trp to native rIDO caused a small (~2−3 nm)

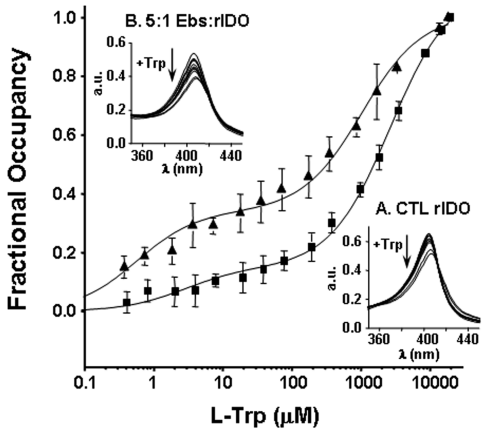

FIGURE 11: Isotherms for binding of L-Trp to native and ebselen-treated rIDO. Fe^{III}-rIDO (~4 μM) was either not treated or treated for 5 min with 5 molar equiv of ebselen followed by removal of any unbound ebselen using a PD Minitrap G-25 gel filtration column. Native rIDO (■) or ebselen-treated rIDO (▲) was then titrated with increasing amounts of L-Trp and the level of substrate binding measured as the extent of change in the absorbance of the heme γ-Soret maxima (i.e., 404 nm for native rIDO and 406 nm for ebselen-treated rIDO). The solid lines represent the nonlinear least-squares fits of the data using a two-independent binding site model. The corresponding UV−visible absorption spectra in the Soret band region for each titration experiment are shown as insets. Only the spectra corresponding to 0.1−1000 molar equiv of L-Trp are shown to preserve clarity. Spectral intensities have been corrected for any dilutions associated with cumulative addition of the L-Trp stock solutions. Data represent means ± the standard deviation of three independent experiments.

bathochromic shift and a pronounced intensity decrease of the heme γ-Soret absorption band (Figure 11, inset A). The binding isotherm was best fit with a model of two independent binding sites with corresponding dissociation constants K_{S1} of 2.7 ± 0.9 μM and K_{S2} of 2.65 ± 0.22 mM (Figure 11). The existence of a second binding site in IDO has also been reported previously (*30*). Titration of L-Trp with ebselen-treated rIDO also revealed a slight (~2−3 nm) bathochromic shift and intensity decrease of the γ-Soret band of the heme due to L-Trp binding (Figure 11, inset B). The binding isotherm fit a model of two independent binding sites with corresponding dissociation constants K_{S1} of 0.57 ± 0.17 μM and K_{S2} of 1.04 ± 0.20 mM (Figure 11). Thus, compared to the native enzyme, treatment with ebselen enhanced the binding of L-Trp to both binding sites of rIDO. Treatment of rIDO with 3 molar equiv of ebselen resulted in binding that was intermediate between that observed with no treatment and treatment with 5 molar equiv of ebselen (data not shown). These data show that despite inhibiting enzyme activity, ebselen enhances the nonproductive binding of L-Trp to rIDO.

Ebselen Reduces the Helical Content and Stability of the rIDO Protein. CD spectroscopy was performed on rIDO with and without ebselen treatment to determine the effect of the drug on the protein secondary structure. The CD spectrum of untreated rIDO displays a pattern that indicates significant α-helical content (Figure 12). Quantitative fitting of the spectrum yielded a prediction of 67% helical content for the rIDO protein, which is in good agreement with previous crystal structure (*34*) and CD (*35*) studies. Treatment of rIDO with 5 molar equiv of ebselen resulted in a spectrum that when fitted indicated a total helical content of 53%, which is significantly lower than that for the native protein (Figure 12). The same ebselen-treated and native rIDO samples were also subjected to thermal denaturation.

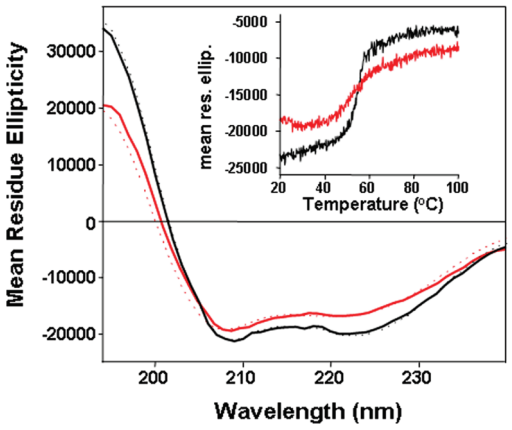

FIGURE 12: Circular dichroism spectra of Fe^{III}-rIDO and effect of ebselen treatment. The CD spectrum of Fe^{III}-rIDO is shown as the black solid curve, and the best fit using CDPro is shown as the black dotted curve. The CD spectrum of Fe^{III}-rIDO following treatment with 5 molar equiv of ebselen for 5 min is shown as the red solid curve along with the CDPro best fit (red dotted curve). The thermal denaturation curves for the two samples are shown in the inset graph in matching colors. Results are representative of three independent experiments.

Loss of structure was monitored at 222 nm over the temperature range of 20−100 °C (Figure 12, inset). The thermal melting curve for the ebselen-treated rIDO sample was significantly shallower than that obtained for the native enzyme sample, indicating that ebselen treatment caused a significant destabilization of the overall rIDO protein structure. The T_m values for untreated and ebselen-treated rIDO were determined to be 56 and 50 °C, respectively. Treatment of rIDO with 3 molar equiv of ebselen resulted in helical content changes and a T_m that was intermediate between that observed with no treatment and treatment with 5 molar equiv of ebselen (data not shown). Together, these data support the possibility that modification of IDO cysteines with ebselen significantly alters the protein secondary structure, which has important implications for substrate binding, active site heme, and enzyme activity.

DISCUSSION

This study identifies ebselen as a potent inhibitor of human IDO. The drug acts by reacting with enzyme cysteine residues which alters the protein conformation and the active site heme environment, resulting in disruption of the substrate binding pocket and an increased level of nonproductive L-Trp binding.

Ebselen exhibits strong electrophilicity that underlies its ability to covalently react with protein cysteine residues to form selenyl−sulfide bonds (*22*). Our studies support the possibility that this electrophilicity allows ebselen to react with multiple cysteine residues of IDO, and this represents the primary mechanism by which ebselen inhibits enzyme activity. Thus, prevention of reaction with cysteine residues and breakage of the selenyl−sulfide bonds both attenuated the ability of ebselen to perturb the heme environment and inhibit enzyme activity. These findings, for the first time, provide a direct link between modification of IDO cysteine residues and alteration of the active site heme environment leading to inhibition of enzyme activity. They also support the possibility that IDO is subject to redox control through modification of cysteine residues.

Depending on the dose employed, ebselen can react with all eight cysteine residues of rIDO. Thus, treatment with ≥10 molar equiv of ebselen resulted in a complete loss of MPB-reactive cysteine residues, and this correlated with changes in the molecular mass of rIDO indicative of eight molecules of bound ebselen. Of note, ebselen binding to rIDO was heterogeneous and hence complex; addition of 4 molar equiv of ebselen did not show a single mass species but rather revealed rIDO species indicative of binding of two to six molecules of ebselen (Figure 5). This indicates that the efficacy with which ebselen reacts with cysteine residues of rIDO varies between different protein molecules. This could be explained if the initial reaction of ebselen with more susceptible cysteine residues of rIDO causes a change in the protein's conformation such that otherwise inaccessible cysteine residues become more available for reaction with ebselen. The heterogeneity and complexity surrounding the action of ebselen make it difficult to accurately determine the number of cysteine residues with which the selenazal drug needs to react to cause complete inhibition. Thus, while ∼50−80% inhibition of enzyme activity was achieved with treatment of rIDO with 4−6 molar equiv of ebselen, mass spectrometry data revealed that the drug reacted with two to seven enzyme cysteine residues over this concentration range (Figures 4 and 5). Our data do indicate, however, that treatment of rIDO with ≥10:1 molar equiv of ebselen results in the maximal binding of the drug to all eight cysteine residues (Figure 5), and this affords >95% inhibition of enzyme activity (Figure 4).

The recently published crystal structure study reveals that human IDO contains two α-helical domains of large and small size (*34*). The helices of the large domain create a cavity for the active site heme, while the small domain covers the top of this cavity. The eight cysteine residues of human IDO are present in both the large (i.e., Cys^{206}, Cys^{335}, Cys^{272}, Cys^{308}, and Cys^{159}) and small domains (i.e., Cys^{112}, Cys^{85}, and Cys^{129}) of the enzyme (*34*). None of these cysteine residues appears to be involved in the catalytic reaction mechanism of the enzyme. Of the eight cysteine residues, only Cys^{129}, which resides within the distal heme pocket, is in the proximity of the active site heme (>10 Å), and mutation of this residue does not result in alteration of enzyme activity (*34*). This supports the possibility that ebselen does not inhibit IDO activity by reacting with specific cysteine residue(s) involved in the catalytic reaction. Instead, our data support the idea that the cysteine residues in IDO are positioned in the protein such that their modification with ebselen induces a significant reduction in the enzyme's total α-helical content and protein stability. Ebselen most likely induces this significant alteration in protein secondary structure as it possesses two bulky, hydrophobic aromatic groups capable of reducing the local hydrophilicity of the protein at the site of attachment and introducing steric bulk. Therefore, we propose that the inhibitory action of ebselen is not due to reaction with specific, catalytically crucial cysteine residue(s) but instead reflects a dose-dependent, cumulative introduction of increased hydrophobicity and/or steric bulk into the IDO protein at the site of cysteine residues, and this leads to the observed dose-dependent alterations in secondary protein structure, perturbation of the active site heme, and resultant inhibition of enzyme activity. In support of this proposal, our findings show that inhibition of enzyme activity, reaction with IDO cysteines, alteration of both the active site heme and protein secondary structure, and promotion of nonproductive substrate binding all follow dose-dependent relationships with ebselen.

Ebselen exhibited a tight binding mode of inhibition of rIDO as evidenced by the low value (∼90 nM) for the observed inhibition constant, which was comparable to the enzyme

concentration employed (50 nM). This is consistent with ebselen covalently binding to cysteine residues of rIDO to form a stable selenyl−sulfide bond. Indeed, in the absence of strong reducing agents, ebselen-treated and gel-filtered rIDO (to remove unbound ebselen) remained inactive for several hours.

Our data show that prior addition of excess GSH abrogates the ability of ebselen to inhibit rIDO. This suggests that ebselen may not effectively inhibit IDO in cells that contain millimolar concentrations of GSH. However, treatment of intact cells with ebselen significantly decreases the cellular content of protein thiols (*22*). Also, this study shows that ebselen, even at low micromolar concentrations, effectively inhibits IDO activity in IFNγ-stimulated human macrophages, which express high levels of active IDO (*11*). These findings may relate to a study showing that ebselen is in dynamic equilibrium with accessible protein thiol groups when GSH is present (*36*), supporting the possibility that the drug can exchange between GSH and the cysteine residues of cellular proteins, including IDO.

The prosthetic heme is critical for IDO activity. In this study, we show that binding of ebselen to cysteine residues inhibits enzyme activity by altering the heme environment of IDO. For Fe^{III}-rIDO, ebselen induced a transition from a high-spin form to a low-spin form. A similar transition is observed when L-Trp binds to the Fe^{III} enzyme. Previously, we showed that this spin state transition is the result of an equilibrium shift between distal heme-bound water and hydroxide ion (*26*). A similar shift from distal water to hydroxide ion ligand may occur when ebselen reacts with rIDO, although the possible cause of this was not determined in this study. The CD data indicated that ebselen induces a significant protein conformational change. This change may cause a basic amino acid residue in the distal pocket to move closer to the distal water ligand to extract a proton. Alternatively, the spin state change may be caused by a change in the properties of the proximal iron−histidine bond as a result of the protein conformational change.

The RR spectroscopic data for the Fe^{II}−CO complex of rIDO with and without bound L-Trp (Figure 10) suggest that ebselen caused a significant enlargement or opening of the distal heme pocket. Studies on a wide variety of CO−heme complexes have established a strong correlation between ν_{Fe-CO} and the polarity and stericity of the distal pocket (*26*, *37*). A decrease in ν_{Fe-CO} is associated with a less polar and/or more open distal pocket. The RR data showed a pronounced decrease in ν_{Fe-CO} from 511 to 500 cm^{-1} as a result of ebselen treatment in the absence of L-Trp (Figure 10A). In the presence of L-Trp, ebselen caused an even greater decrease in ν_{Fe-CO} from 537 to 497 cm^{-1} (Figure 10B). Significantly, the RR spectra of the Fe^{II}−CO rIDO complex with and without L-Trp appear almost identical following treatment with 5 molar equiv of ebselen (cf. two bottom spectra of Figure 10). This indicates that either with or without L-Trp the CO ligand experiences almost the same distal pocket environment following ebselen treatment of rIDO. As L-Trp and CO tightly interact in the distal pocket of native rIDO (*26*), this observation suggests that ebselen causes L-Trp and CO to separate in the distal pocket. Assuming L-Trp remains bound after ebselen treatment, this would suggest that the distal pocket opens as a result of the protein conformational changes indicated by the CD data.

Substrate binding studies showed that ebselen enhanced the ability of L-Trp to bind to rIDO. This is conceivable if ebselen causes the distal binding pocket to open, allowing L-Trp to bind nonspecifically, i.e., in random orientations. We propose that this is important for the inhibition of rIDO activity by ebselen. To date, site-directed mutagenesis of rIDO has failed to identify any amino acid residue crucial for catalytic activity except those that are essential for heme binding (*25*, *34*, *38*, *39*). Thus, it appears the major catalytic strategy of IDO is one of reactant proximity; IDO employs tight control over substrate position, orientation, and coordination with respect to the heme iron-bound distal oxygen in the active site to catalyze the reaction. Therefore, the mechanism by which ebselen inhibits rIDO involves initial reaction with multiple enzyme cysteine residues, which causes a conformational change and disruption of the substrate binding pocket, loss of substrate specificity, and an increased level of nonproductive substrate binding.

In light of the evidence of IDO expression contributing to a pathological state of immune tolerance toward certain tumor-associated antigens, there is growing interest in the discovery of potent small molecule inhibitors of IDO activity, as such agents may represent effective adjuvants for traditional chemotherapeutic agents (*4*, *5*). The most commonly employed inhibitor, 1-methyltryptophan, represents a relatively inefficient inhibitor exhibiting a K_i of 34 μM (*6*). Recent studies report that naphthoquinone-based drugs (*8*) and exiguamine-based drugs (*7*) represent potent, uncompetitive inhibitors of IDO that exhibit K_i values in the low nanomolar range. Our study highlights the fact that ebselen also represents a potent nanomolar-range inhibitor and therefore represents one of the most efficient small molecule inhibitors of IDO activity reported to date. While the mechanism(s) by which naphthoquinone and exiguamine drugs inhibit IDO is yet to be fully elucidated, our study demonstrates that targeting IDO cysteine residues represents a novel strategy for potently inhibiting enzyme activity. While ebselen is not expected to be selective for IDO in vivo, our study suggests that further work aimed at the development of potent selenazal-based inhibitors with enhanced specificity for IDO that can be tested for their propensity to inhibit the enzyme in vivo is warranted.

In conclusion, this study shows that ebselen is a potent inhibitor of IDO and establishes that the integrity of IDO cysteine residues is crucial for the maintenance of protein secondary structure, active site heme environment, and enzyme activity. The study highlights that although no amino acid residues are directly required for the catalytic reaction, targeting IDO cysteine residues represents an effective and novel means of inhibiting enzyme activity and supports the possibility that IDO is subject to redox control through cysteine modification. The extent to which IDO represents a target for ebselen and other selenazal-based drugs in vivo warrants investigation.

REFERENCES

1. Thomas, S. R., and Stocker, R. (1999) Redox reactions related to indoleamine 2,3-dioxygenase and tryptophan metabolism along the kynurenine pathway. *Redox Rep. 4*, 199–220.
2. Mellor, A. L., and Munn, D. H. (2004) IDO expression by dendritic cells: Tolerance and tryptophan catabolism. *Nat. Rev. Immunol. 4*, 762–774.
3. King, N. J., and Thomas, S. R. (2007) Molecules in focus: Indoleamine 2,3-dioxygenase. *Int. J. Biochem. Cell Biol. 39*, 2167–2172.
4. Muller, A. J., and Prendergast, G. C. (2005) Marrying immunotherapy with chemotherapy: Why say IDO? *Cancer Res. 65*, 8065–8068.
5. Muller, A. J., DuHadaway, J. B., Donover, P. S., Sutanto-Ward, E., and Prendergast, G. C. (2005) Inhibition of indoleamine 2,3-dioxygenase, an immunoregulatory target of the cancer suppression gene Bin1, potentiates cancer chemotherapy. *Nat. Med. 11*, 312–319.
6. Cady, S. G., and Sono, M. (1991) 1-Methyl-DL-tryptophan, β-(3-benzofuranyl)-DL-alanine (the oxygen analog of tryptophan), and β-[3-benzo(b)thienyl]-DL-alanine (the sulfur analog of tryptophan) are competitive

inhibitors for indoleamine 2,3-dioxygenase. *Arch. Biochem. Biophys. 291*, 326–333.
7. Brastianos, H. C., Vottero, E., Patrick, B. O., Van Soest, R., Matainaho, T., Mauk, A. G., and Andersen, R. J. (2006) Exiguamine A, an indoleamine-2,3-dioxygenase (IDO) inhibitor isolated from the marine sponge *Neopetrosia exigua*. *J. Am. Chem. Soc. 128*, 16046–16047.
8. Kumar, S., Malachowski, W. P., DuHadaway, J. B., LaLonde, J. M., Carroll, P. J., Jaller, D., Metz, R., Prendergast, G. C., and Muller, A. J. (2008) Indoleamine 2,3-dioxygenase is the anticancer target for a novel series of potent naphthoquinone-based inhibitors. *J. Med. Chem. 51*, 1706–1718.
9. Thomas, S. R., Mohr, D., and Stocker, R. (1994) Nitric oxide inhibits indoleamine 2,3-dioxygenase activity in interferon-γ primed mononuclear phagocytes. *J. Biol. Chem. 269*, 14457–14464.
10. Thomas, S. R., Terentis, A. C., Cai, H., Takikawa, O., Levina, A., Lay, P. A., Freewan, M., and Stocker, R. (2007) Post-translational regulation of human indoleamine 2,3-dioxygenase activity by nitric oxide. *J. Biol. Chem. 282*, 23778–23787.
11. Thomas, S. R., Salahifar, H., Mashima, R., Hunt, N. H., Richardson, D. R., and Stocker, R. (2001) Antioxidants inhibit indoleamine 2,3-dioxygenase in IFN-γ-activated human macrophages: Posttranslational regulation by pyrrolidine dithiocarbamate. *J. Immunol. 166*, 6332–6340.
12. Sies, H. (1993) Ebselen, a selenoorganic compound as glutathione peroxidase mimic. *Free Radical Biol. Med. 14*, 313–323.
13. Schewe, T. (1995) Molecular actions of ebselen: An antiinflammatory antioxidant. *Gen. Pharmacol. 26*, 1153–1169.
14. Nakamura, Y., Feng, Q., Kumagai, T., Torikai, K., Ohigashi, H., Osawa, T., Noguchi, N., Niki, E., and Uchida, K. (2002) Ebselen, a glutathione peroxidase mimetic seleno-organic compound, as a multifunctional antioxidant. Implication for inflammation-associated carcinogenesis. *J. Biol. Chem. 277*, 2687–2694.
15. Chew, P., Yuen, D. Y., Koh, P., Stefanovic, N., Febbraio, M. A., Kola, I., Cooper, M. E., and de Haan, J. B. (2009) Site-specific antiatherogenic effect of the antioxidant ebselen in the diabetic apolipoprotein E-deficient mouse. *Arterioscler. Thromb. Vasc. Biol. 29*, 823–830.
16. Yamaguchi, T., Sano, K., Takakura, K., Saito, I., Shinohara, Y., Asano, T., and Yasuhara, H. (1998) Ebselen in acute ischemic stroke: A placebo-controlled, double-blind clinical trial. Ebselen Study Group. *Stroke 29*, 12–17.
17. Saito, I., Asano, T., Sano, K., Takakura, K., Abe, H., Yoshimoto, T., Kikuchi, H., Ohta, T., and Ishibashi, S. (1998) Neuroprotective effect of an antioxidant, ebselen, in patients with delayed neurological deficits after aneurysmal subarachnoid hemorrhage. *Neurosurgery 42*, 269–286.
18. Maiorino, M., Roveri, A., Coassin, M., and Ursini, F. (1988) Kinetic mechanism and substrate specificity of glutathione peroxidase activity of ebselen (PZ51). *Biochem. Pharmacol. 37*, 2267–2271.
19. Morgenstern, R., Cotgreave, I. A., and Engman, L. (1992) Determination of the relative contributions of the diselenide and selenol forms of ebselen in the mechanism of its glutathione peroxidase-like activity. *Chem.-Biol. Interact. 84*, 77–84.
20. Zhao, R., Masayasu, H., and Holmgren, A. (2002) Ebselen: A substrate for human thioredoxin reductase strongly stimulating its hydroperoxide reductase activity and a superfast thioredoxin oxidant. *Proc. Natl. Acad. Sci. U.S.A. 99*, 8579–8584.
21. Cotgreave, I. A., Duddy, S. K., Kass, G. E., Thompson, D., and Moldeus, P. (1989) Studies on the anti-inflammatory activity of ebselen. Ebselen interferes with granulocyte oxidative burst by dual inhibition of NADPH oxidase and protein kinase C. *Biochem. Pharmacol. 38*, 649–656.
22. Sakurai, T., Kanayama, M., Shibata, T., Itoh, K., Kobayashi, A., Yamamoto, M., and Uchida, K. (2006) Ebselen, a seleno-organic antioxidant, as an electrophile. *Chem. Res. Toxicol. 19*, 1196–1204.
23. Walther, M., Holzhutter, H. G., Kuban, R. J., Wiesner, R., Rathmann, J., and Kuhn, H. (1999) The inhibition of mammalian 15-lipoxygenases by the anti-inflammatory drug ebselen: Dual-type mechanism involving covalent linkage and alteration of the iron ligand sphere. *Mol. Pharmacol. 56*, 196–203.
24. Zembowicz, A., Hatchett, R. J., Radziszewski, W., and Gryglewski, R. J. (1993) Inhibition of endothelial nitric oxide synthase by ebselen. Prevention by thiols suggests the inactivation by ebselen of a critical thiol essential for the catalytic activity of nitric oxide synthase. *J. Pharmacol. Exp. Ther. 267*, 1112–1118.
25. Littlejohn, T. K., Takikawa, O., Truscott, R. J., and Walker, M. J. (2003) Asp274 and His346 are essential for heme binding and catalytic function of human indoleamine 2,3-dioxygenase. *J. Biol. Chem. 278*, 29525–29531.
26. Terentis, A. C., Thomas, S. R., Takikawa, O., Littlejohn, T. K., Truscott, R. J., Armstrong, R. S., Yeh, S. R., and Stocker, R. (2002) The heme environment of recombinant human indoleamine 2,3-dioxygenase. Structural properties and substrate-ligand interactions. *J. Biol. Chem. 277*, 15788–15794.
27. Sono, M. (1989) The roles of superoxide anion and methylene blue in the reductive activation of indoleamine 2,3-dioxygenase by ascorbic acid or by xanthine oxidase-hypoxanthine. *J. Biol. Chem. 264*, 1616–1622.
28. Sono, M., Taniguchi, T., Watanabe, Y., and Hayaishi, O. (1980) Indoleamine 2,3-dioxygenase. Equilibrium studies of the tryptophan binding to the ferric, ferrous, and CO-bound enzymes. *J. Biol. Chem. 255*, 1339–1345.
29. Copeland, R. A. (2000) Enzymes, 2nd ed., Wiley-VCH, New York.
30. Sono, M. (1989) Enzyme kinetic and spectroscopic studies of inhibitor and effector interactions with indoleamine 2,3-dioxygenase. 2. Evidence for the existence of another binding site in the enzyme for indole derivative effectors. *Biochemistry 28*, 5400–5407.
31. Sreerama, N., and Woody, R. W. (2000) Estimation of protein secondary structure from circular dichroism spectra: Comparison of CONTIN, SELCON, and CDSSTR methods with an expanded reference set. *Anal. Biochem. 287*, 252–260.
32. Sreerama, N., Venyaminov, S. Y., and Woody, R. W. (2000) Estimation of protein secondary structure from circular dichroism spectra: Inclusion of denatured proteins with native proteins in the analysis. *Anal. Biochem. 287*, 243–251.
33. Harris, D., and Loew, G. (2003) Mechanistic origin of the correlation between spin state and spectra of model cytochrome P450 ferric heme proteins. *J. Am. Chem. Soc. 115*, 5799–5802.
34. Sugimoto, H., Oda, S., Otsuki, T., Hino, T., Yoshida, T., and Shiro, Y. (2006) Crystal structure of human indoleamine 2,3-dioxygenase: Catalytic mechanism of O_2 incorporation by a heme-containing dioxygenase. *Proc. Natl. Acad. Sci. U.S.A. 103*, 2611–2616.
35. Austin, C. J., Astelbauer, F., Kosim-Satyaputra, P., Ball, H. J., Willows, R. D., Jamie, J. F., and Hunt, N. H. (2009) Mouse and human indoleamine 2,3-dioxygenase display some distinct biochemical and structural properties. *Amino Acids 36*, 99–106.
36. Ullrich, V., Weber, P., Meisch, F., and von Appen, F. (1996) Ebselen-binding equilibria between plasma and target proteins. *Biochem. Pharmacol. 52*, 15–19.
37. Vetter, S. W., Terentis, A. C., Osborne, R. L., Dawson, J. H., and Goodin, D. B. (2009) Replacement of the axial histidine heme ligand with cysteine in nitrophorin 1: Spectroscopic and crystallographic characterization. *J. Biol. Inorg. Chem. 14*, 179–191.
38. Papadopoulou, N. D., Mewies, M., McLean, K. J., Seward, H. E., Svistunenko, D. A., Munro, A. W., and Raven, E. L. (2005) Redox and spectroscopic properties of human indoleamine 2,3-dioxygenase and a His303Ala variant: Implications for catalysis. *Biochemistry 44*, 14318–14328.
39. Chauhan, N., Basran, J., Efimov, I., Svistunenko, D. A., Seward, H. E., Moody, P. C., and Raven, E. L. (2008) The role of serine 167 in human indoleamine 2,3-dioxygenase: A comparison with tryptophan 2,3-dioxygenase. *Biochemistry 47*, 4761–4769.